Numerical Simulation of Foam Formation and Evolution with Modified Cellular Automata

C. Körner, R. F. Singer
WTM Institute, Department of Materials Science, University of Erlangen, Germany

Abstract

A numerical model based on the cellular automaton technique has been developed to simulate the formation and evolution of metal foam produced from metal powder mixed with a blowing agent. The model incorporates the influence of surface tension, gas atmosphere, gas pressure and viscosity. It is able to reproduce qualitatively the pore structure found in experiments. The model has been used successfully to demonstrate the effect of important process features such as foaming velocity, mould confinement, hydrogen loss and gas pressure.

1 Introduction

The cell structure of metal foams produced from metal powder mixed with a foaming agent is strongly dependent on the foaming conditions. The investigation of the formation and evolution of the cellular structure is important since it determines the properties, especially the mechanical properties, of the metal foam. The present understanding of the influence and the mutual interaction of foaming time, temperature, atmospheric pressure, gravitational force, viscosity of the melt, surface tension etc. is rather poor and mainly grounded on empirical knowledge. The elucidation and quantitative description of the physical mechanisms controlling the formation of metal foams is essential for designing foaming technologies and alloys.
During each phase of formation - bubble nucleation, growth, coarsening and coalescence - the metal foam is a non-equilibrium system due to the interfacial energy of the gas-liquid interface. That is, the cellular structure is intrinsically unstable and always evolving towards patterns with less surface area unless other factors such as boundary pinning or short-range repulsive forces intervene. The basic mechanism to reduce the interfacial area is the elimination of entire cells, i.e. the foam coarsens. Considerable theoretical work has been carried out on the description of the evolution of dry foams [1] [2]. These models investigate the temporal evolution of an already existing cellular structure. They are not able to describe the expansion of the foam starting from the nucleation of bubbles. For this reason, the influence of processing parameters on the resulting cellular structures can not be inferred from these models. In the present paper a modified Cellular Automaton (CA) model is suggested that is able to model the complete foam formation and evolution process with aluminium and TiH_2 as the matrix and the foaming agent, respectively.

2 Physical Model

It is assumed in our model that nuclei for bubbles are already present at the beginning in form of micro cracks and small pores. Additionally, bubbles can develop due to nucleation within the liquid metal. Nucleation within the liquid metal requires bubble hydrogen pressures in the

J. Banhart, M.F. Ashby, N.A. Fleck: *Metal Foams and Porous Metal Structures.* © MIT Verlag (1999)

range of 10-100 bar for aluminium corresponding to critical hydrogen concentrations ranging from c_{crit} = $6 \cdot 10^{-6}$ to $2 \cdot 10^{-5}$ mol/cm^3 [3]. We assume that the decomposition of the TiH_2-particles can be treated as a homogenous volume source Q of hydrogen in the liquid metal. This is reasonable since the mean distance of two TiH_2-particles is only about 30 - 40 µm. Due to the high diffusion velocity of hydrogen in molten aluminium [4] concentration gradients on this length scale are completely equalised within 10^{-3} s. This is short compared to the decomposition time of the TiH_2. The situation is illustrated in Fig. 1 where $c(\underline{x}, t)$ is the hydrogen concentration throughout the melt resulting from the decomposition of the TiH_2 and diffusion of hydrogen to the gas bubbles. The hydrogen concentration adjacent to a gas bubble according to Sieverts' law [3] is denoted by c_b. As long as $c(\underline{x}, t)$ is smaller than c_{crit} nucleation within the liquid metal does not occur. If the local hydrogen concentration exceeds c_{crit} a new bubble nucleus is formed.

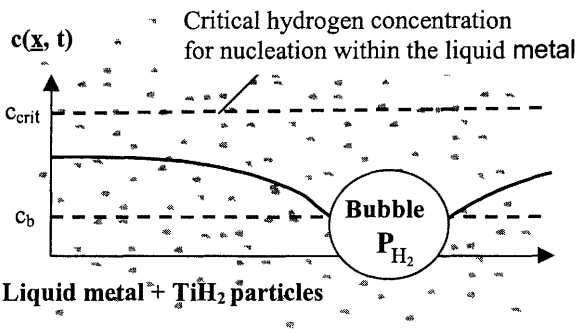

Fig. 1: Schematic representation of the hydrogen concentration $c(\underline{x}, t)$ as a function of the distance to a bubble.

Let us now consider foam formation in a two-dimensional spatial region Ω. Zones within Ω where there is metal are denoted by ω. Gas is found in the region $\Omega \setminus \omega$. The metal-gas interface is denoted by $\Gamma(t)$. $\Gamma(t)$ consists of the surface of the individual bubbles and that of ω. During heating the foaming agent decomposes and the released hydrogen diffuses to the bubble nuclei. The rising bubble pressure P_{H_2} forces the bubble to expand. The gas flux from the metal into the bubbles is governed by the following equations:

i) gas diffusion equation

$$\frac{\partial c(\underline{x},t)}{\partial t} + \underline{v} \cdot \nabla c(\underline{x},t) - \nabla(D \nabla c(\underline{x},t)) = Q(\underline{x},t) \quad for \quad \underline{x} \in \omega \setminus \Gamma(t)$$

(c: hydrogen concentration, D: diffusion coefficient, Q: hydrogen source, $\underline{v}$: diplacement velocity, T: absolute temperature)

ii) Sieverts' law (for hydrogen dissolved in liquid aluminium [3])

$$c_b(\underline{x},t) = 1.4 \cdot 10^{-3} \cdot 10^{-\frac{2760}{T}} \cdot \sqrt{P_{H_2}} \frac{mol}{cm^3 \sqrt{bar}} \quad for \quad \underline{x} \in \Gamma(t)$$

Movement of the interface $\Gamma(t)$

In our model the displacement of $\Gamma(t)$ results on the one hand from the expansion of the whole system and on the other hand from the local growth of the individual bubbles. The global expansion is described as follows. The movement of $\Gamma(t)$ changes the bubble area, i.e. bubbles grow or shrink. In order to fulfil global mass conservation the displacement field $\underline{u}(\underline{x},t)$ defined on ω has to be divergence free, i.e. $\nabla u(\underline{x},t) = 0$. We describe the material flow due to bubble expansion with the help of fundamental solutions of the last equation. Within this framework growing and shrinking bubbles are modelled by point sources and sinks located at the centre of mass of the bubbles, respectively. The displacement increment $d\underline{u}$ for bubble j is given by

$$d\underline{u} = \frac{1}{2\pi} \sum_{i \neq j} S_i \frac{\underline{x}_j - \underline{x}_i}{|\underline{x}_j - \underline{x}_i|^2}$$

(S_i: source amplitude of bubble number i)

for an infinite spatial region Ω. With additional mirror sources other boundary conditions can be realised.

For the local contribution to du we assume equilibrium of the local acting forces on $\Gamma(t)$. If the distance to other bubbles is large bubble growth is that of an isolated bubble in a liquid. The gas-liquid interface $\Gamma(t)$ of a bubble is given by:

$$P_{H_2} - P_0 - P_\sigma - P_\eta = 0 \qquad on \quad \Gamma(t) \quad with \quad P_\sigma = \frac{\sigma}{R} = \sigma \cdot \kappa \qquad P_\eta = \xi \cdot \eta \cdot \frac{dR}{dt}$$

(P_0: atmospheric pressure, P_{H_2} : bubble pressure, σ: surface tension, η: viscosity, R: curvature radius, κ: curvature , ξ: constant)

The situation changes if the bubble density is so high that the bubbles are no more able to assume their energetically favourable round shape without deforming other bubbles. Due to the increase of total surface area mutually repulsive forces proportional to the surface tension develop. In this case P_0 in the upper equation is replaced by $\tilde{P}_{H_2} - \tilde{P}_\sigma$ where $\tilde{P}_{H_2}$ is the bubble pressure of the neighbouring bubble and $\tilde{P}_\sigma$ is the Laplace pressure at the surface of the neighbouring bubble nearest to the point of interest.

3 Cellular Automaton Model

Cellular automata (CA) are mathematical models designed to describe a complex interaction of a large number of subsystems called cells. These cells all follow the same rules and interact only in the *local* neighbourhood with other cells. Due to the fact that our model for bubble formation and evolution separates the local growth of the bubbles from the global expansion of the whole system a CA model can be used. Our approach is very similar to the well known activator–inhibitor models [5] with the bubble pressure as activator and the presence of other bubbles in the neighbourhood as inhibitor.

The growth process is realised in our CA model as follows. The spatial region Ω is represented by an array of regularly arranged rectangular cells. Each cell is characterised by three variables: the volume fraction of fluid ε, the concentration of the dissolved hydrogen c, the number of the bubble the cell belongs to and a state – boundary and non-boundary - containing information whether the cell is considered to change the value of liquid fraction during the next simulation step.

The calculation of the curvature κ and the interface normal vector $\underline{n}$ is crucial and must be carried out carefully in order to eliminate the artificial anisotropy caused by the rectangular cells. We regard a 36-neighbour surrounding of a cell whose state variable indicates that it can change their liquid fraction during the next simulation step (see Figure 2). The curvature κ of an interface cell with the solid fraction ε is calculated from the following expression:

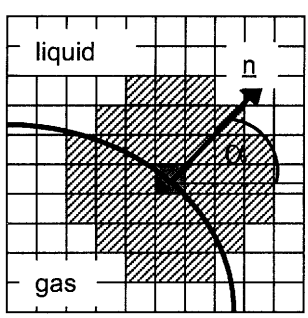

Fig. 2: 36-neighbour surrounding of a cell at the gas-liquid boundary.

$$\kappa = \frac{18.5 - 3.5 \cdot C + 7 \cdot (1-\varepsilon) \cdot C - G}{18.5 \cdot a} \quad with \quad C = \begin{cases} \sin\alpha & \alpha \geq \frac{\pi}{4} \\ \quad for & \\ \cos\alpha & \alpha < \frac{\pi}{4} \end{cases}$$

(G: total gas fraction within the 36-surrounding, a: cell size, α: angle between normal vector and horizontal lattice axis)

This formula is a modification of the method proposed by Dithey et al. [6] where $C = 1$. Without the correction factor C bubble shape is not round in equilibrium. An explicit finite difference scheme was used to solve the gas diffusion equation with the middle points of the cells as finite difference mesh. The modification of the liquid fraction increment during a simulation step is described in the following way:

$$\Delta\varepsilon = \begin{cases} (\underline{n} \cdot d\,\underline{u}) \cdot \cos\alpha & 0 \le \alpha \le \frac{\pi}{4} \\ \qquad\qquad for & \\ (\underline{n} \cdot d\,\underline{u}) \cdot \sin\alpha & \frac{\pi}{4} < \alpha \le \frac{\pi}{2} \end{cases}$$

Again it is essential to take the orientation of the CA lattice explicitly into account in order to eliminate the anisotropy induced by the quadratic lattice.

4 Results and Discussion

As long as nothing else is indicated the following material parameters were used below:
$a = 50\ \mu m$, $T = 700\ ^{\circ}C$, $D = 4 \cdot 10^{-3}\ cm^2/s$, $\sigma = 2 \cdot 10^{-5}\ J/cm^2$, $\xi \cdot \eta = 100\ g/cm\ s$, $P_0 = 1\ bar$.

Effect of Confinement
Our analytical method to calculate the displacement field $\underline{u}$ allows to investigate two situations: a) confined expansion with rectangular boundaries and b) free expansion in a semi-infinite spatial region. The resulting cell structures are depicted in Fig. 3.

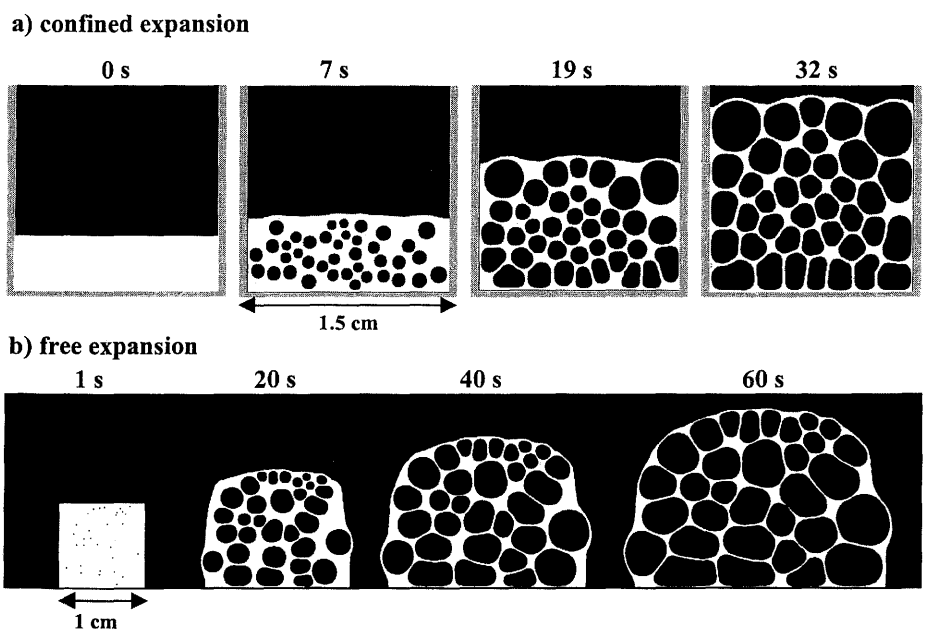

Fig. 3: Temporal evolution of cell morphology for a) confined (300 x 300 CA cells) and b) free expansion (800 x 600 CA cells). Material parameters: $Q = 1.3 \cdot 10^{-6}\ mol/cm^3 s$, $P_0 = 1\ bar$ (hydrogen atmosphere)

If the expansion is free the bubbles are statistically orientated. The temporal evolution shows that there are only few topological rearrangements. In contrast, the confined expansion leads to elongated bubbles in the foaming direction. In order to keep the surface energy low many topological rearrangements take place. The different bubble size results from the statistically distributed bubble nuclei. The bubbles are large in the end if the initial nuclei density was low and vice versa. Coarsening due to the pressure difference between bubbles of different size is very slow and has no significant influence within the time frame investigated.

Foaming Velocity

Since our model at the moment does not allow to vary the temperature we modelled the influence of the heating velocity by altering the hydrogen source Q. If Q is small the released hydrogen has enough time to diffuse to the preexistent bubble nuclei thus keeping $c < c_{crit}$. In this case bubble nucleation from the liquid metal is suppressed. For higher heating velocities it happens that the local hydrogen concentration exceeds c_{crit} and new bubble nuclei evolve (Fig.4).

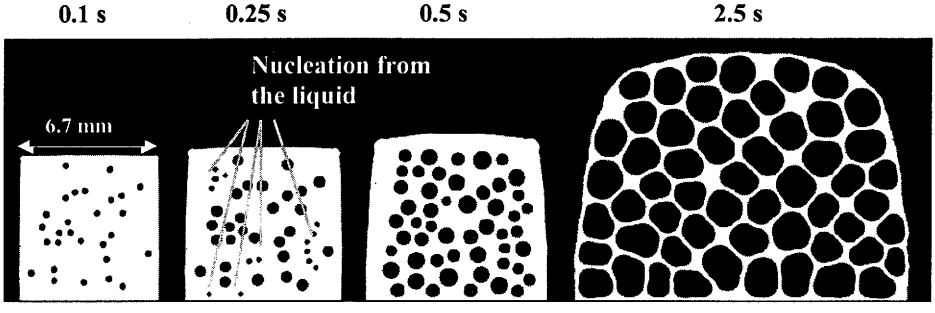

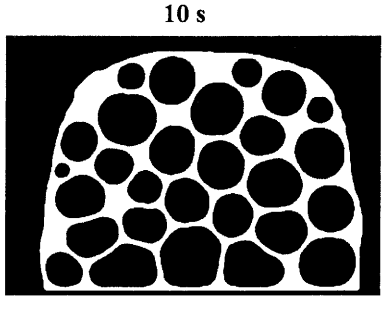

Fig. 4: Influence of the foaming velocity on the resulting cell structure (450 x 280 CA cells, c_{crit}= 10^{-5} *mol/cm*^{3}, 28 statistically distributed initial nuclei, P_0 = *1 bar*, hydrogen partial pressure = *0 bar*) :
above: $Q=1.3\cdot10^{-5}$ *mol/cm*^{3}*s*, number of bubbles has doubled
right: same initial state but $Q=3.9\cdot10^{-6}$ *mol/cm*^{3}*s*, number of bubbles is equal to the number of initial nuclei, bubbles at the surface shrink due to loss of hydrogen to the surroundings.

In regions where the bubble density is low c increases until c_{crit} is reached and a new bubble nucleus is borne. In this way nucleation from the liquid metal equalises large bubble density differences. Consequently, the bubble size and its variation decreases with increasing foaming velocity.

Hydrogen loss at the surface

How much hydrogen is lost during foaming depends on the hydrogen partial pressure in the atmosphere and the ratio of surface area to volume. It is also a function of the foaming velocity. If the decomposition of the TiH_2 is very slow there is much time for the dissolved hydrogen to diffuse to the surface and to be unavailable for foaming. For high decomposition rates and nucleation from the liquid, the local hydrogen gradient always points to the next

bubble. Hydrogen diffuses first to the growing bubbles rather than to the surface. Nevertheless, the hydrogen loss per time interval in absolute terms is higher than for slow foaming conditions. Fig. 5 shows the temporal evolution of the cell structure if we assume $P_{H_2} = 0$ at the surface.

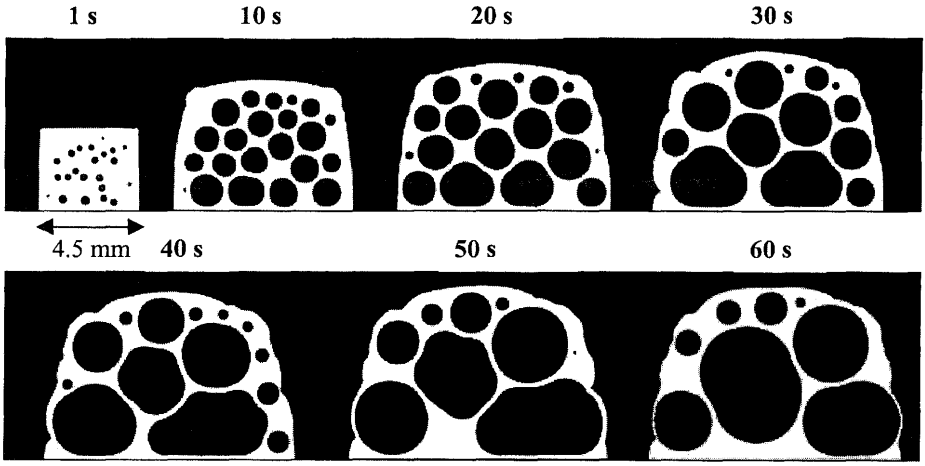

Fig. 5: Effect of hydrogen loss on the cell structure (300 x 150 CA cells, $Q = 2.6 \cdot 10^{-6}$ $mol/cm^3 s$). 22 statistically distributed bubble nuclei. $P_{H_2} = 0$ bar at the surface.

Bubbles near to the surface eventually shrink and vanish due to the high hydrogen loss to the surroundings. Consequently, the cell structure coarsens. Another effect is that the growing velocity of the foam approaches approximately zero 40 s after the beginning of foaming.

Atmospheric Pressure

The bubble pressure is only slightly higher than P_0. Consequently, if we increase P_0 without altering other parameters, the residual bubble volume decreases and vice versa.

References

[1] Glazier, J.A., Weaire, D., *The kinetics of cellular patterns*, J. Phys.: Condens. Matter **4,** 1867-1894 (1992)

[2] Stavans, J., *The evolution of cellular structures*, Review, Rep. Prog. Phys. **56** , 733-789 (1993)

[3] Gerhardt, M., Schuster, H., *Das digitale Universum: Zellulare Automaten als Modelle der Natur*, Vieweg (1995)

[4] Eichenauer, W., Markopoulus, J., *Messung des Diffusionskoeffizienten von Wasserstoff in flüssigem Aluminium*, **65**, 649-652 (1974)

[5] Lutze, P., Ruge, J., *Wasserstoff in Aluminium und seinen Legierungen*, METALL, 44. Jahrgang, Heft 8, pp. 741-748 (1990)

[6] Dilthey, U., Pavlik, V., Reichel, T., *Numerical Simulation of Dendritic Solidification with Modified Cellular Automata*, in: Mathematical Modelling of Weld Phenomena 3 (Ed. Cerjak, H.), Institute of Materials, 85-105 (1996)